Author Manuscript

Author Manuscript

Author Manuscript

Author Manuscript

HHS Public Access

Author manuscript

FASEB J. Author manuscript; available in PMC 2022 April 01.

Published in final edited form as:

FASEB J. 2021 April ; 35(4): e21463. doi:10.1096/fj.202002590RRR.

Organ-on-chip of the cervical epithelial layer: A platform to study normal and pathological cellular remodeling of the cervix

Ourlad Alzeus G. Tantengco[1,2], **Lauren S. Richardson**[1,3], **Paul Mark B. Medina**[2], **Arum Han**[3], **Ramkumar Menon**[1]

[1]Division of Maternal-Fetal Medicine and Perinatal Research, Department of Obstetrics and Gynecology, The University of Texas Medical Branch at Galveston, Galveston, TX, USA

[2]Department of Biochemistry and Molecular Biology, College of Medicine, University of the Philippines Manila, Manila, Philippines

[3]Department of Electrical and Computer Engineering, Department of Biomedical Engineering, Texas A&M University, College Station, TX, USA

Abstract

Damage to the cervical epithelial layer due to infection and inflammation is associated with preterm birth. However, the individual and/or collective roles of cervical epithelial layers in maintaining cervical integrity remain unclear during infection/inflammation. To determine the intercellular interactions, we developed an organ-on-chip of the cervical epithelial layer (CE-OOC) composed of two co-culture chambers connected by microchannels, recapitulating the ectocervical and endocervical epithelial layers. Further, we tested the interactions between cells from each distinct region and their contributions in maintaining cervical integrity in response to LPS and TNFα stimulations. The co-culture of ectocervical and endocervical cells facilitated cellular migration of both epithelial cells inside the microchannels. Compared to untreated controls, both LPS and TNFα increased apoptosis, necrosis, and senescence as well as increased pro-inflammatory cytokine productions by cervical epithelial cells. In summary, the CE-OOC established an in vitro model that can recapitulate the ectocervical and the endocervical epithelial regions of the cervix. The established CE-OOC may become a powerful tool in obstetrics and gynecology research such as in studying cervical remodeling during pregnancy and parturition and the dynamics of cervical epithelial cells in benign and malignant pathology in the cervix.

Correspondence Ramkumar Menon, Division of Maternal-Fetal Medicine and Perinatal Research, Department of Obstetrics and Gynecology, The University of Texas Medical Branch at Galveston, 301 University Blvd., Galveston, TX 77555-1062, USA., ra2menon@utmb.edu.

AUTHOR CONTRIBUTIONS

O.A.G. Tantengco conducted the experiments. O.A.G. Tantengco and L. Richardson performed data analysis and drafted the manuscript. R. Menon conceived the project, designed the experiments, and provided funding. R. Menon, A. Han, and P.M. Medina helped with data analysis and interpretation, and prepared the manuscript.

SUPPORTING INFORMATION

Additional Supporting Information may be found online in the Supporting Information section.

CONFLICT OF INTEREST

The authors state no conflicts of interest regarding this study

Author Manuscript Author Manuscript Author Manuscript Author Manuscript

Keywords

cervix; cervical ripening; epithelial-to-mesenchymal transition; organ-on-a-chip; pregnancy; preterm birth

1 | INTRODUCTION

The uterine cervix is an important organ during gestation and keeps the developing fetus *in utero* until term delivery. It is composed of two cellular compartments: the epithelial and the stromal layer. The epithelial layer lining the cervical canal is divided into three distinct regions: the ectocervix, the transformation zone, and the endocervix, while the stromal layer is composed mainly of the extracellular matrix (ECM) incorporating fibroblasts, immune, and smooth muscle cells.[1,2] The cervix undergoes remodeling so it can remain intact and closed throughout pregnancy to maintain the fetus within the uterus and prevent preterm birth.[3] This process is characterized by changes in the epithelial, stromal, immune, and endothelial cell function in the cervix as well as changes in the composition and structure of the ECM.[4] The aberrant timing of cervical ripening is one of the major causes of preterm birth.[5,6] Infection and inflammation during pregnancy can hasten the cervical ripening process, promote the influx of immune cells, and increase inflammation, which can lead to preterm birth.

Cervical remodeling during pregnancy is divided into four distinct but overlapping phases: softening, ripening, dilation, and postpartum repair.[7] Cervical remodeling starts with softening which is a slow and progressive decrease in tissue stiffness without the loss of tensile strength.[8] Cervical ripening occurs before uterine contractions of labor and involves a decrease in collagen concentration and increase in collagen solubility. The structural integrity and tensile strength of the cervix are lost during this phase in preparation for the third phase which is cervical dilation. This is the opening of the cervix in response to uterine contractions of labor. It is usually characterized by increased inflammation and leukocyte recruitment in the cervix.[4] After delivery, the postpartum repair takes place immediately which involves rapid increases in repair processes, relief of mechanical stretch, and decrease in inflammatory responses in the cervix.[1]

Epithelial cells play an important role in maintaining the overall health of the cervix since they are involved in remodeling and growth throughout pregnancy.[9] These epithelial cells line the cervical lumen which creates a barrier protecting the stroma from pathogens present in the lower reproductive tract (Figure 1A). They also secrete cytokines and chemokines that attract and activate inflammatory cells and antimicrobial factors that can kill any invading pathogens.[7] Any compromise in the cervical epithelial layer can induce cervical remodeling, leading to preterm birth.[10,11] In previous studies using traditional 2D in vitro cultures and animal models (eg, mouse), it was shown that infection and inflammation can cause damage to the cervical epithelial layer, accelerate cervical ripening, and promote preterm birth.[12–14] Damage to the cervical epithelium also promotes ascending infection, intrauterine inflammation, and the induction of preterm birth.[15]

Author Manuscript Author Manuscript Author Manuscript Author Manuscript

The use of traditional 2D cell culture systems gave us insightful data on the role of the cervical epithelial layer in cervical remodeling. However, these systems are limited for replicating the in vivo physiological environment and cannot provide a better understanding of these processes because each cell type (ectocervical, transformation zone, and endocervical epithelial cells) is studied independently, while intercellular interactive properties and impacts are not considered.[16,17] In vivo, it is believed that these three different cell types interact to protect the amniotic cavity from ascending infections originating in the vagina.[3,18] Thus, the lack of cellular interactions in traditional 2D culture is a major limitation, making it difficult to understand the role of the distinct regions of the cervical epithelial layer in cervical remodeling. While in vivo animal models provide a useful understanding of cervical remodeling during pregnancy, animal experiments do not often translate to replication in humans and are very expensive.[19–21] One way to address these challenges is using a microfluidic-based compartmentalized co-culture system that mimics the complex multi-cellular structure of human organs. Such organ-on-chip (OOC) devices can better mimic the physiological conditions and responses of human organ systems, thus bridging the gap between 2D/mixed cell culture models, animal models, and human-based s tudies.[22]However, although some OOC models that mimic the feto-maternal interface of humans have been developed recently,[16,23,24] OOC models for the cervix are still lacking.

To overcome the limitations associated with in vitro and in vivo models, we developed a two-chamber organ-on-chip for cervical epithelial layer (CE-OOC) that allowed the co-culture of ectocervical and endocervical epithelial cells in two different but interconnected microenvironments. Using the CE-OOC, we tested the effects of lipopolysaccharide (LPS), mimicking bacterial infection, and tumor necrosis factor alpha (TNFα), mimicking inflammation, on cell death, cell migration, epithelial-to-mesenchymal transition (EMT), and the secretion of inflammatory cytokines by ectocervical and endocervical epithelial cells.

2 | METHODS

2.1 | Institutional review board approval

This study used immortalized cervical epithelial cells provided by Dr. Richard Pyles (The University of Texas Medical Branch at Galveston, TX, USA). No subject recruitment or tissue collection was performed for this study, and thus, the study was designated as exempt by the UTMB Institutional Review Board (IRB).

2.2 | Human cervical epithelial cell culture

The immortalized ectocervical and endocervical epithelial cells used in this study were previously characterized and were shown to have conserved toll-like receptor (TLR) expression when compared to primary ectocervical and endocervical epithelial cells.[25,26] The cells were immortalized by transduction with PA317/LXSN-16 E6E7-conditioned medium (HPV16 E6/E7 immortalization) and cultured in keratinocyte serum-free medium (KSFM) (37010022; Thermo Fisher Scientific), a culture medium that is highly selective for epithelial cells, supplemented with bovine pituitary extract (30 μg/mL), epidermal growth

Author Manuscript Author Manuscript Author Manuscript Author Manuscript

factor (0.1 ng/mL), $CaCl_2$ (0.4 mM), and primocin (0.5 mg/mL) (ant-pm-1; Invivogen; San Diego, CA) at 37°C in a 5% CO_2 environment, and grown to 80% confluence.

2.3 | Microfluidic CE-OOC design

The microfabrication procedure is similar to that described previously for the amnion membrane-OOC device.[23] In short, to form the master mold, a 2-step photolithography process was conducted using photosensitive epoxy (SU-8; MicroChem, Westborough, MA, USA) forming the first microchannel layer (5-μm-deep microchannels) and the second cell culture chamber layer (500-μm-deep cell culture chambers). The master mold was then coated with (tridecafluoro-1,1,2,2-tetrahydrooctyl) trichlorosilane (United Chemical Technologies, Bristol, PA, USA) to facilitate polydimethylsiloxane (PDMS) release from the master mold after replication. A soft lithography technique was utilized to make the CE-OOCs out of PDMS. PDMS devices were replicated from the master mold by pouring PDMS prepolymer (10:1 mixture, Sylgard 184; DowDuPont, Midland, MI, USA) onto the mold, followed by curing at 85°C for 45–60 minutes. The reservoirs to hold culture medium were punched out from this PDMS layer using a 4 mm diameter punch bit (Syneo, Angleton, TX, USA) mounted on a drill press. This PDMS layer was treated with oxygen plasma (Harrick Plasma, Ithaca, NY, USA) for 90 seconds to improve the bonding of the PDMS layer onto the glass substrate and to also make the device hydrophilic for easy cell and culture medium loading, followed by bonding onto a glass substrate (22 × 22 mm). A single device (2 cm × 2 cm) fits within a well of a 6-well culture plate.

2.4 | CE-OOC device preparation for Matrigel filling of the microchannels

Before using the CE-OOC, the devices were washed with 70% ethanol for 10 minutes for sterilization, washed 3 times with 1× phosphate-buffered saline (PBS), and then the microchannels were coated with Matrigel (Corning Matrigel Basement Membrane Matrix, DEV-free; 1:4 in KSFM) by loading Matrigel to the outer chamber of the CE-OOC and applying suction pressure from the inner chamber through a p1000 pipette tip attached to a vacuum system. The device was then incubated overnight at 37°C in a 5% CO_2 environment.

2.5 | Cell seeding and culture in the CE-OOC

After overnight coating with Matrigel, the devices were washed 3 times with complete KSFM before cell seeding. Ectocervical and endocervical epithelial cells were trypsinized and seeded into the CE-OOC: 200 000 ectocervical epithelial cells were loaded into the outer chamber (136 μm^2), and 75 000 endocervical epithelial cells were loaded into the inner chamber (28 μm^2) of the CE-OOC. Seeding densities were determined based on previous cell loading titrations. The CE-OOCs were incubated at 37°C with 5% CO_2 for 24 hours (h) and then stained with live cell dyes for nucleus (NucBlue Live ReadyProbes for ectocervical epithelial cells and NucRed Live 647 ReadyProbes for endocervical epithelial cells) following the protocol provided by the company (R37605 and R37106 Thermo Fisher Scientific, Waltham, MA, USA). After staining, the cells were exposed to different localized chemical treatments, as described below.

Author Manuscript Author Manuscript Author Manuscript Author Manuscript

2.6 | Analyzing cell migration in response to infection and inflammation

To test the effects of infection and inflammation on cellular transition in cervical epithelial cells, we treated the CE-OOC with one of the following conditions for 96 hours: (1) KSFM (control); (2) 100 ng/mL LPS diluted in KSFM; and (3) 100 ng/mL TNFα diluted in KSFM. These concentrations were selected as they are within the range that is seen in the amniotic fluid of women with infection-associated pregnancy complications, and were also used successfully in our previous studies.[27,28]

To compare the effect of co-culture vs. monoculture in the cell migration, CE-OOC devices where only one cell type is loaded into a chamber while the other chamber remains empty, designated here as monoculture condition, were also tested. Once cells reached 70–80% confluence in each chamber, each CE-OOC was rinsed with sterile 1× PBS and treated with the respective conditions (LPS or TNFα, as described above), and incubated at 37°C, in 5% CO_2 and 95% humidity conditions, for 96 hours.

For both co-culture and monoculture CE-OOC devices, after 96 hours of chemical treatment, bright-field microscopy (Nikon Eclipse TS100 microscope, 310 magnification; Nikon, Tokyo, Japan) or fluorescence microscopy (Keyence All-in-One Fluorescence Microscope-BZ-X810) was performed to determine cell morphology and to count the number of cells that migrated through the microchannels to the other side of the chamber.

2.7 | Immunocytochemical localization of intermediate filaments cytokeratin and vimentin

2.7.1 | Cell staining—Immunocytochemical staining for vimentin (3.7 μL/mL; ab92547; Abcam, Cambridge, MA, USA) and cytokeratin-18 (CK-18; 1 μL/mL; ab668; Abcam) was performed after 96 hours, as previously described.[26,29] Manufacturer's instructions were used to calculate the staining dilutions to ensure uniform staining. After 96 hours, cells were fixed with 4% paraformaldehyde, permeabilized with 0.5% Triton X, and blocked with 3% bovine serum albumin in 1× PBS, prior to incubation with primary antibodies overnight at 4°C. After washing with 1× PBS, the CE-OOCs were incubated with Alexa Fluor 488– and 594–conjugated secondary antibodies (Thermo Fisher Scientific) diluted 1:400 in 1× PBS for 2 hours in the dark. The CE-OOCs were washed with 1× PBS, and then also treated with NucBlue Fixed ReadyProbes Reagent (R37606; Thermo Fisher Scientific, Waltham, MA) to stain the nucleus.

2.8 | Apoptosis/Necrosis staining

To monitor for apoptosis and necrosis, after 96 hours treatment of the CE-OOC, some devices were stained for apopto sis and necrosis markers. The devices were first washed with cold PBS for 10 minutes. Then, the apoptosis/necrosis staining was conducted using the Alexa Fluor 488 Annexin V/Dead Cell Apoptosis Kit (V13241, Invitrogen, Carlsbad, CA). The staining solution was prepared by adding 5 μL Alexa Fluor 488 Annexin V and 1 μL propidium iodide to 100 μL Annexin binding buffer. The outer chamber was filled with 160 μL, while the inner chamber was filled with 65 μL of the staining solution. The devices were incubated at room temperature for 1 hours with constant rocking. The devices were then washed 3 times with 1× PBS for 10 minutes with constant rocking. The cells were fixed with 4% paraformaldehyde, permeabilized with 0.5% Triton X, washed 3 times with 1× PBS, and

Author Manuscript Author Manuscript Author Manuscript Author Manuscript

then treated with NucBlue Fixed Cell Stain ReadyProbes Reagent (R37606; Thermo Fisher Scientific, Waltham, MA), before being imaged using fluorescence microscopy.

2.9 | Image analysis

Three random regions of interest per CE-OOC were used to determine red (CK-18) and green (vimentin) fluorescence intensity, and Annexin V and propidium iodide staining. Uniform laser settings, brightness, contrast, and collection settings were also used for all images collected. Images were not modified for intensity analysis. ImageJ software was used to measure vimentin and CK-18 staining intensity from 3 different regions per treatment condition. Image analysis was conducted in six biological replicates for all cell experiments.

2.10 | Cytological senescence-associated β-galactosidase (SA β-Gal) assay

To assess for senescence, SA β-gal staining was conducted using a commercial histochemical staining assay, following the manufacturer's instructions (CS0030–1 KT; Sigma-Aldrich, Inc.; St. Louis, MO).[30] Briefly, cells cultured in CE-OOC were washed twice with 1× PBS, fixed for 6–7 minutes with the provided Fixation Buffer, washed again with 1× PBS, and incubated overnight at 37°C with fresh β-Gal staining solution. Following incubation, cells were evaluated using a standard light microscope.

2.11 | Milliplex luminex assays for inflammatory cytokine markers analyses

To analyze inflammation, the cytokines interleukin-6 (IL-6) and interleukin-8 (IL-8) were analyzed from the cell supernatants in the CE-OOC. Supernatants were manually collected from the reservoirs of both chambers after 96 hours of treatment. Milliplex assays were performed with IL-6 and IL-8 antibody-coated beads (HCYTOMAG-60 K; Merck, Darmstadt, Germany). Standard curves were developed with duplicate samples of known quantities of recombinant proteins that were provided by the manufacturer. Sample concentrations were determined by relating the absorbance values that were obtained to the standard curve by linear regression analysis.

2.12 | Statistical analyses

All data were analyzed using Prism 7 software (GraphPad Software, La Jolla, CA, USA). The Shapiro-Wilk test for normality was conducted to check for the normality of the data. Student's *t* test was used to compare results with two means. Ordinary one-way analysis of variance followed by the Tukey's multiple comparison test was used to compare normally distributed data with at least three means. The Kruskal-Wallis test with Dunn's multiple comparison test was used for data that were not normally distributed. Asterisks denote *P* values as follows: $*P < .05$; $**P < .01$; $***P < .001$, and $***P < .0001$.

3 | RESULTS

3.1 | CE-OOC development

The CE-OOC design represents the three distinct regions of the cervical epithelium (Figure 1A). It is composed of two circular chambers, the outer chamber (marked as blue color in Figure 1D) for ectocervical epithelial cell culture and the inner chamber (marked as yellow

Author Manuscript Author Manuscript Author Manuscript Author Manuscript

color in Figure 1D) for endocervical epithelial cell culture, connected by an array of microfluidic channels filled with type IV collagen where the cells can migrate (Figure 1B). The outer and inner chambers had heights of 500 μm (inner chamber volume: 14 000 μm^3, outer chamber volume: 68 000 μm^3) and were connected by 24 microchannels (5 μm in height, 30 μm in width, 600 μm in length; Figure 1C).

The two culture compartments connected by the array of microchannels could maintain their respective culture environment, as can be seen by the clear separation of the two colors (Figure 1D), where the inner endocervical epithelial cell culture chamber was filled with yellow-colored dye and the outer ectocervical epithelial cell culture chamber was filled with blue-colored dye. The developed CE-OOC provided an environment that was conducive to the growth and proliferation of cervical epithelial cells. Image analysis of the cells cultured in the CE-OOC revealed that cervical epithelial cells reached 90%–100% confluence in the CE-OOC within one day of culture (Figures 1E and S1). Immunocytochemical staining showed that both ectocervical and endocervical epithelial cells exist in a metastate, since these cells expressed both epithelial and mesenchymal markers, CK-18, and vimentin, respectively (Figure 1E). No cross-contamination between the ectocervical and endocervical epithelial cell populations after cell seeding into the CE-OOC was observed (Figure S2).

3.2 | LPS and TNFα induce changes in monocultured cervical epithelial cell morphology and migration

Monocultures of ectocervical and endocervical epithelial cells reached confluence within 96 hours (Figure 2A, B control). Cells also entered and migrated through the microchannels filled with type IV collagen and exited the microchannel into the opposite culture compartments within 96 hours of culture (Figure 3A, C). Ectocervical epithelial cells showed a more fibroblastoid morphology as they migrated through the microchannels (Figure 3A), while endocervical epithelial cells showed an increase in cell area and pseudopod (arm-like projection of cell membrane that are developed in the direction of movement) formation (Figure 3C) as they traveled through the microchannels. Interestingly, the cells reverted to their epithelial morphology upon reaching the other chamber of the CE-OOC. Under normal conditions, endocervical epithelial cells showed a higher migratory potential compared to ectocervical epithelial cells (3-fold higher, Figure 3B, D).

To determine the effects of infection and inflammation on the cervical epithelial cells in the CE-OOC, we treated these cells with either LPS or TNFα for 96 hours and checked for changes in cell morphology, migration capability, and intermediate filament expression. LPS and TNFα promoted pseudopod formation in migrating endocervical epithelial cells inside the microchannels (Figure S4A,B). LPS treatment for 96 hours also increased the cell migratory potentials (Figure 3B, D LPS). TNFα treatment for 96 hours slightly increased the migration of ectocervical epithelial cells and slightly diminished the migration of endocervical epithelial cells (Figure 3 TNFα).

Author Manuscript Author Manuscript Author Manuscript Author Manuscript

3.3 | Characteristics of cellular transition in the CE-OOC under normal, infectious, and inflammatory conditions

3.3.1 | Innate transition properties of ectocervical and endocervical epithelial cells—

To show cellular transition in the CE-OOC, we used fluorescence microscopy to show changes in the expression of intermediate filaments as the cell migrates from one chamber to the other. The migration of ectocervical and endocervical epithelial cells under control conditions revealed an increase in the expression of vimentin (green) as the cells migrate through the microchannels (Figure 4A, B control). Once the ectocervical and endocervical epithelial cells reached the outer chamber, they revert to the baseline vimentin:CK-18 ratio. These results show that ectocervical and endocervical cells undergo EMT as they migrate through the microchannels, and then undergo mesenchymal-to-epithelial transition (MET) once they exit the microchannels to an adjacent chamber (Figure 4A, B control). In a separate experiment, we have shown the tissue remodeling properties of endocervical cells using scratch assays where a wound (induced by scratch) is healed through the cyclic transition of endocervical cells.[25] Thus, data from the presented OOC studies confirm the results that have already been seen.

3.3.2 | LPS- and TNFα-induced EMT in ectocervical and endocervical epithelial cells—

To show how LPS and TNFα impact cell migration and transition in the CE-OOC, we exposed the cells to LPS and TNFα for 96 hours and documented the changes in intermediate filaments as the cells migrate through the microchannels. LPS and TNFα treatments increased the vimentin:CK-18 ratios (Figure S3A, B) in both the ectocervical and endocervical epithelial cells compared with the cells under standard cell culture conditions. TNFα also increased the vimentin:CK-18 ratio of ectocervical and endocervical epithelial cells (Figure S3A, B). The increase in vimentin expression signified that cells start to acquire a more mesenchymal phenotype. This indicates that the chronic exposure of cells to LPS may induce EMT in cervical epithelial cells.

A static state of EMT (irreversible mesenchymal state) was observed, as shown by persistently elevated levels of vimentin (green), in both the ectocervical (Figure 4A) and endocervical epithelial cells (Figure 4B) treated with LPS and TNFα. The cells, regardless of whether they are inside the chambers or microchannels, had elevated vimentin:CK-18 ratios (one- to twofold increase from the untreated control, data not shown). We did not observe MET, even when cells exited the microchannels to the adjacent side/chamber.

3.4 | Cell fate of co-cultured ectocervical and endocervical epithelial cells in CE-OOC under normal, infectious, and inflammatory conditions

Before analyzing how co-culture in CE-OOC impacts the cell fates of ectocervical and endocervical epithelial cells, we first performed fluorescence staining to assess apoptosis and necrosis, and the SA β-Gal assay to detect senescence in monoculture in CE-OOC. LPS and TNFα significantly increased the number of late apoptotic and necrotic cells compared to untreated cells (LPS vs. control: $P < .05$; TNFα vs. control: $P < .05$) (Figure S5A,B). LPS and TNFα also significantly increased senescence in monocultured ectocervical (control vs. LPS: $P < .01$; control vs. TNFα: $P < .01$) and endocervical epithelial cells (control vs. LPS:

Author Manuscript Author Manuscript Author Manuscript Author Manuscript

$P < .0001$; control vs. TNFα: $P < .001$) compared to untreated cells in CE-OOC (Figure S6A).

The same experiments on apoptosis, necrosis, and senescence were performed in co-culture set-up in the CE-OOC. A decrease in live ectocervical epithelial cells (cells stained with blue, DAPI) was observed upon treatment with LPS ($P < .05$) and TNFα ($P < .05$) compared to untreated cells. Early apoptotic [cells stained with DAPI (blue) and Annexin V (green)] ectocervical epithelial cells increased by 1.8-fold with LPS treatment and 2.6-fold with TNFα treatment compared to untreated cells. Both LPS and TNFα significantly increased the late apoptotic [cells stained with DAPI (blue), Annexin V (green), and propidium iodide (red)] and necrotic [cells stained with DAPI (blue) and propidium iodide (red)] ectocervical epithelial cells ($P < .01$ and $P < .05$, respectively). For endocervical epithelial cells (Figure 5B), LPS and TNFα significantly decreased live cells compared to the control ($P < .05$ and $P < .001$, respectively). LPS and TNFα significantly increased the number of late apoptotic and necrotic cells compared to untreated cells ($P < .01$). Our data showed more pronounced effects of LPS and TNFα on apoptosis and necrosis when ectocervical and endocervical cells are co-cultured in the CE-OOC.

Under normal culture conditions, senescence was observed in both ectocervical and endocervical epithelial cells after 96-h incubation in the CE-OOC (Figure 5C). Both LPS and TNFα significantly increased the number of senescent ectocervical (control vs. LPS: $P < .01$; control vs. TNFα: $P < .05$) and endocervical epithelial cells (control vs. LPS: $P < .05$; control vs. TNFα: $P < .05$) compared to untreated cells (Figure 5C). Senescence was also observed among ectocervical and endocervical cells migrating in the microchannels (Figure S6B,C). We observed the differential effects of LPS and TNFα on the cell fate of ectocervical and endocervical epithelial cells. Infection and inflammation both induced apoptosis and necrosis in ectocervical and endocervical epithelial cells; however, a higher level of senescence was observed in ectocervical epithelial cells (LPS: 9.66 ± 1.03%; TNFα: 8.37 ± 0.78%) compared to endocervical epithelial cells (LPS: 6.29 ± 0.97%; TNFα: 6.35 ± 0.70%). These results suggest that the CE-OOC can be used to study cell fate of cervical epithelial cells.

3.5 | Characteristics of co-cultured ectocervical and endocervical epithelial cells in the CE-OOC

To create an in vitro set-up that can recapitulate the in vivo conditions of the cervical epithelial layer, we performed co-culture experiments of ectocervical and endocervical epithelial cells in the CE-OOC to determine the dynamics of the different regions of the cervical epithelial layer. Crystal violet staining confirmed that both cell types remain viable after 96 hours of culture in the CE-OOC (Figure S1). To determine the effect of co-culture conditions on cell migration, we labeled the ectocervical epithelial cells using a blue nuclear dye and the endocervical epithelial cells using a yellow nuclear dye, and tracked the cells for 96 hours. To determine how infectious and inflammatory stimuli affect the cervical epithelial layer, we treated each chamber with LPS and TNFα (Table 1) and compared the results to an untreated control.

Author Manuscript Author Manuscript Author Manuscript Author Manuscript

Under untreated co-culture conditions, few ectocervical and endocervical epithelial cells migrated into the microchannels (Figure 6A). In general, we did not observe a complete migration to the adjacent chamber. Instead, the ectocervical and endocervical epithelial cells migrated and met inside the microchannels (Figure 6A). These migrating cells still retained their epithelial morphology. This migratory pattern is different from those seen in the monoculture condition (Figure 3), where ectocervical or endocervical epithelial cells could migrate all the way to the other compartment. LPS treatment in the outer chamber (ectocervix chamber) increased the migration of both ectocervical and endocervical epithelial cells. However, LPS treatment in the inner chamber (endocervix chamber) only increased the migration of endocervical epithelial cells and did not affect the migration of the ectocervical epithelial cells in the outer chamber (Figure 6B,C). This result suggests that the infection in the ectocervical epithelium may already have influenced the endocervical epithelium. This also further supports the findings reported above (monoculture case) suggesting that LPS increases cervical epithelial cell migration.

The total number of migrated cells significantly decreased in the co-culture set-up compared with the monoculture experiments (8–23 migrated cells in monoculture [Figure 3] versus 1–6 migrated cells in co-culture [Figure 6]). This may be because the opposite compartment is empty in monoculture set-up and allows easier cellular migration, while the opposite compartment is filled with cells in the case of co-culture, making it difficult for cells to completely migrate. This, along with increased paracrine signaling from interacting cells in the co-culture condition, may have also contributed to the decreased cell migration. Interestingly, when LPS was added to both chambers, we did not observe an increase in the number of migrating cells in either chamber compared to the control (Figure 6B). This could be explained by the increase in apoptosis, necrosis, and senescence caused by simultaneous LPS treatments in both chambers, which can hinder the cells from migrating.

In the CE-OOC, when ectocervical compartment was treated with TNFα, endocervical epithelial cells from the adjacent compartment migrate toward the ectocervical compartment. Similarly, when endocervical compartment was treated with TNFα, ectocervical epithelial cells from the adjacent compartment migrated toward the endocervical compartment. This may be a mechanism responsible for maintaining the cervical epithelial layer. When TNFα was applied in both chambers, we did not observe a change in the number of migrating cells from both chambers compared to the control (Figure 6C).

3.6 | Propagation of inflammatory mediators in the CE-OOC

To determine the inflammatory response of co-cultured ectocervical and endocervical epithelial cells against infectious and/or inflammatory stimuli, we analyzed the presence of IL-6 and IL-8 in the culture supernatant in the CE-OOC. Endocervical epithelial cells have higher baseline IL-6 (8-fold) and IL-8 ($P < .05$) production compared to ectocervical epithelial cells (Figure 7A, B). In all the treatment conditions, IL-6 and IL-8 released from endocervical epithelial cells treated with LPS or TNFα, regardless of which chamber they were applied to, were higher compared to ectocervical epithelial cells.

Author Manuscript Author Manuscript Author Manuscript Author Manuscript

Generally, LPS and TNFα treatment in either the inner or the outer chamber increased IL-8 production in ectocervical epithelial cells but did not affect IL-8 production in endocervical epithelial cells (Figure 7D, F). However, treatment of the inner chamber with TNFα increased IL-6 production in endocervical epithelial cells (Figure 7E). LPS treatment in both chambers increased IL-8 production by ectocervical epithelial cells, while TNFα treatment in both chambers increased the production of IL-6 and IL-8 in both cervical epithelial cells (Figure 7C-F). These results show that exposure of cells in the CE-OOC to infectious and/or inflammatory stimuli can promote the production of inflammatory cytokines (Figure 7G). Infection or inflammation in one region of the cervical epithelial layer may propagate the inflammatory response that could inflict damage on other regions of the cervix.

4 | DISCUSSION

This CE-OOC was developed to study the cellular interaction, migration, and transition of epithelial cells from each distinct zone of the cervical epithelial layer. Based on our findings, we determined that: (1) both ectocervical and endocervical epithelial cells express epithelial and mesenchymal markers, indicating that these cells are in a metastate; (2) cervical epithelial cells can transition and migrate through the type IV collagen-filled microchannel; (3) some migrating ectocervical epithelial cells acquire a fibroblastoid morphology as they cross the microchannels, but most retain their epithelial morphology throughout their migration period; (4) some migrating endocervical epithelial cells formed pseudopods as they migrate through the microchannels; (5) LPS and TNFα induced a static (irreversible) state of EMT, promoted cell migration, and stimulated inflammatory cytokine production; (6) LPS and TNFα significantly decreased cell viability and increased late apoptosis and necrosis in co-cultured ectocervical and endocervical epithelial cells; (7) co-culture experiments showed that cervical epithelial cells can migrate through the collagen-filled microchannels, remain there, and integrate with each other. These migrating cell populations in the microchannels may suggest the formation of the transformation zone, which is composed mainly of cells from the endocervix migrating toward the ectocervix and transitioning into a squamous morphology, as seen in vivo; and (8) under co-culture conditions, LPS treatment promoted cell migration and inflammatory cytokine production, while TNFα treatment only increased inflammatory cytokine production without enhancing cell migration.

Two microfluidic human cervix-on-a-chip models have been previously reported. The one from Huh & Seo is a transwell device composed of an upper compartment containing cervical epithelial cells and a lower compartment where cervical stromal cells and vascular endothelial cells can be cultured.[32] This model allows cervical stromal-epithelial cell interactions: however, some limitations of the transwell system include difficulty in the local application of stimuli to only one compartment, and limited imaging of cellular migrations. Another cervix-OOC utilized a planar design that allows both ectocervical and endocervical epithelial cells to grow in two chambers connected by a single microchannel to allow the formation of the squamo-columnar junction.[33] Our CE-OOC supplements these two previous models and provides better intercellular interactions, offers sensitive measurement capabilities of membrane permeability and biomolecule propagation, and allows real-time imaging of cellular processes.[23] Lack of complete formation of the squamo-columnar

Author Manuscript Author Manuscript Author Manuscript Author Manuscript

junction observed in our study could also be considered as a limitation of our horizontal model. We speculate that prolonged incubation or changes in culture environment may help to recreate such features.

Our study provides a new approach for studying cellular processes and paracrine signaling in the cervical epithelial layer under normal, infection, and/or inflammatory conditions through a new in vitro model. This allows us to further understand the important functions of the cervical epithelial layer and its implications in the cervical remodeling process during pregnancy. The cervical epithelial layer secretes cytokines and chemokines, which can recruit and activate inflammatory cells that can kill invading pathogens.[7] These epithelial cells have tight junctions that seal off intercellular spaces to prevent any pathogens from infecting the cervix. The ectocervix is lined by a stratified, squamous, non-keratinized epithelium, which offers a protective barrier against pathogens, while the endocervix is lined by a single layer of mucus-secreting columnar epithelium and inhibits the ascent of microbes from the lower genital tract to the fetus.[34] This collective barrier function of the cervical epithelial layer is important for protecting the stromal compartment as the matrix remodels.[1] The individual contribution of the different cellular components of the cervix and their interaction with each other cannot be studied using traditional 2D cell culture methods.

In this study, pathological conditions during pregnancy were recreated by treating cells in the CE-OOC with LPS and TNFα. LPS is an endotoxin of Gram-negative bacteria that is associated with infection-induced preterm labor in humans,[35] while TNFα is significantly elevated in patients presenting with preterm labor, regardless of whether a concomitant intra-amniotic infection is present or not.[36–39] In experiments using the CE-OOC, migration of ectocervical and endocervical epithelial cells through the microchannels increased with LPS and TNFα treatments. Both treatments also increased vimentin expression in these migrating cervical epithelial cells. Vimentin is associated with mesenchymal and leader bleb-based migration, especially in cells migrating through confined spaces.[40,41] These migrating and proliferating cells in the CE-OOC may mimic the postpartum repair of the cervical epithelium to maintain the integrity of the cervical epithelial layer. Our study also suggests that inflammation-induced cervical cell damage at one region of the cervix is likely repairable through migration and proliferation of cells from the other regions; however, damage on both sides is hard to recover or remodel, suggesting a pathological condition.

When one compartment was treated with TNFα, we observed a concomitant increase in migration of cervical epithelial cells from the other compartment toward the treated compartment. We hypothesize that inflammatory stimuli in one area of the cervical epithelial layer send signals to recruit epithelial cells to re-establish homeostasis in the affected areas (here, simulated by TNFα treatment on only one chamber). Such a phenomenon has been reported in the intestinal surface epithelium during epithelial restitution, where TNFα-mediated signaling guides epithelial cells next to the injury to form pseudopodia-like structures and migrate toward the injury site to cover the damaged area.[31] TNFα increases apoptosis, necrosis, and senescence of cervical cells, which can cause tissue injury. Thus, the migration of normal cells from the opposite side toward the TNFα-treated side is likely in response to cyto-attractive messaging between the two chambers. This attraction of normal cells to an injured site could be in response to a cytokine, growth factors, or extracellular

Author Manuscript Author Manuscript Author Manuscript Author Manuscript

vesicle-mediated responses. However, when both compartments were treated with TNFα, there was no increase in cell migration. This can be attributed to increased rates of cell death due to TNFα treatments.

LPS and TNFα increased late apoptosis and necrosis in cervical epithelial cells. This shows that high doses of TNFα can compromise the cervical epithelial layer, probably via the induction of massive inflammation and apoptotic and necrotic cell death, as reported previously in other human cell types.[42,43] While both LPS and TNFα caused a significant increase in apoptosis and necrosis in cervical epithelial cells compared to the untreated control, these cells only represent a small percentage of the cell population and the majority of these cells remain viable and are capable of remodeling.

5 | CONCLUSIONS

In summary, this CE-OOC device developed here allowed us to overcome the limitations of traditional 2D culture. We investigated the interactions of epithelial cells from different zones of the cervical epithelial layer and observed how these cells respond to infection and inflammatory stimuli when cultured as a single unit. However, this model was built to particularly study paracrine signaling, cell death, cell transition and migration, and the inflammatory response of the cervical epithelial layer. Thus, some limitations of this CE-OOC include the lack of cervical stromal cells, as well as different immune cells that greatly contribute to the cervical remodeling process during pregnancy and parturition. Future designs of this model will include cervical stromal cells mixed to complete the entire histological structure of the cervix. Additional chambers to accommodate vaginal epithelial cells and decidual cells can complete the feto-maternal interface from the lower vaginal tract to the fetal membranes. These additions will be useful for studying ascending intra-amniotic infection.

Supplementary Material

Refer to Web version on PubMed Central for supplementary material.

Acknowledgments

Funding information

O Tantengco is an MD-PhD trainee in the MD-PhD in Molecular Medicine Program, supported by the Philippine Council for Health Research and Development, Department of Science and Technology, Republic of the Philippines, and administered through the University of the Philippines Manila. L Richardson is a postdoctoral fellow in the Regulatory Science in Environmental Health and Toxicology Training Grant (T32 ES026568), supported by the National Institute of Environmental Health Sciences (NIEHS) of the National Institutes of Health (NIH) of the United States, administered through Texas A&M University. This study was supported by 1R01HD100729-01 (NIH/NICHD) [R Menon and A Han]).

Abbreviations:

CE-OOC	cervical epithelial layer-Organ-on-chip
CK-18	cytokeratin 18

Author Manuscript Author Manuscript Author Manuscript Author Manuscript

ECM	extracellular matrix
EMT	epithelial-to-mesenchymal transition
IL-6	interleukin 6
IL-8	interleukin 8
KSFM	keratinocyte serum-free medium
LPS	lipopolysaccharide
MET	mesenchymal-to-epithelial transition
OOC	organ-on-chip
PBS	phosphate-buffered saline
PDMS	polydimethylsiloxane
SA β-Gal	senescence-associated β-galactosidase
TLR	toll-like receptor
TNFα	tumor necrosis factor alpha
Vim	vimentin

REFERENCES

1. Mahendroo M. Cervical remodeling in term and preterm birth: insights from an animal model. Reproduction. 2012;143:429–438. [PubMed: 22344465]
2. Payne KJ, Clyde LA, Weldon AJ, Milford T-A, Yellon SM. Residency and activation of myeloid cells during remodeling of the prepartum murine cervix1. Biol Reprod. 2012;87:1–7.
3. Yellon SM. Contributions to the dynamics of cervix remodeling prior to term and preterm birth†. Biol Reprod. 2017;96:13–23. [PubMed: 28395330]
4. Word RA, Li XH, Hnat M, Carrick K. Dynamics of cervical remodeling during pregnancy and parturition: mechanisms and current concepts. Semin Reprod Med. 2007;25:69–79. [PubMed: 17205425]
5. Vink J, Feltovich H. Cervical etiology of spontaneous preterm birth. Semin Fetal Neonatal Med. 2016;21:106–112. [PubMed: 26776146]
6. Vink J, Mourad M. The pathophysiology of human premature cervical remodeling resulting in spontaneous preterm birth: where are we now? Semin Perinatol. 2017;41:427–437. [PubMed: 28826790]
7. Timmons B, Akins M, Mahendroo M. Cervical remodeling during pregnancy and parturition. Trends Endocrinol Metab. 2010;21:353–361. [PubMed: 20172738]
8. Read CP, Word RA, Ruscheinsky MA, Timmons BC, Mahendroo MS. Cervical remodeling during pregnancy and parturition: molecular characterization of the softening phase in mice. Reproduction. 2007;134:327–340. [PubMed: 17660242]
9. Nallasamy S, Mahendroo M. Distinct roles of cervical epithelia and stroma in pregnancy and parturition. Semin Reprod Med. 2017;35:190–199. [PubMed: 28278536]
10. Anton L, Sierra L-J, DeVine A, et al. Common cervicovaginal microbial supernatants alter cervical epithelial function: mechanisms by which lactobacillus crispatus contributes to cervical health. Front Microbiol. 2018;9:1–16. [PubMed: 29403456]

Author Manuscript Author Manuscript Author Manuscript Author Manuscript

11. Anton L, DeVine A, Sierra L-J, Br own AG, Elovitz MA. miR-143 and miR-145 disrupt the cervical epithelial barrier through dysregulation of cell adhesion, apoptosis and proliferation. Sci Rep. 2017;7:1–15. [PubMed: 28127051]
12. Nold C, Anton L, Brown A, Elovitz M. Inflammation promotes a cytokine response and disrupts the cervical epithelial barrier: a possible mechanism of premature cervical remodeling and preterm birth. Am J Obstet Gynecol. 2012;206(208):e1–208.e7.
13. Racicot K, Cardenas I, Wunsche V, et al. Viral infection of the pregnant cervix predisposes to ascending bacterial infection. J Immunol. 2013;191:934–941. [PubMed: 23752614]
14. McGee D, Smith A, Poncil S, Patterson A, Bernstein AI, Racicot K. Cervical HSV-2 infection causes cervical remodeling and increases risk for ascending infection and preterm birth. PLoS ONE. 2017;12:1–15.
15. Pavlidis I, Spiller OB, Sammut Demarco G, et al. Cervical epithelial damage promotes Ureaplasma parvum ascending infection, intrauterine inflammation and preterm birth induction in mice. Nat Commun. 2020;11:1–12. [PubMed: 31911652]
16. Sosa-Hernández JE, Villalba-Rodríguez AM, Romero-Castillo KD, et al. Organs-on-a-Chip Module: A Review from the Development and Applications Perspective, Micromachines. 9 (2018), (no.10,), 536. 10.3390/mi9100536.
17. Niepel M, Hafner M, Mills CE, et al. A multi-center study on the reproducibility of drug-response assays in mammalian cell lines. Cell Syst. 2019;9(35–48):e5.
18. Yellon SM. Immunobiology of Cervix Ripening. Front Immunol. 2020;10:1–19.
19. Stouffer RL, Woodruff TK. Nonhuman primates: a vital model for basic and applied research on female reproduction, prenatal development, and women's health. ILAR J. 2017;58:281–294. [PubMed: 28985318]
20. Grossmann H, Weinbauer GF, Baker A, Fuchs A, Luetjens CM. Enhanced normograms and pregnancy outcome analysis in nonhuman primate developmental toxicity studies. Reprod Toxicol. 2020;95:29–36.
21. Bonney EA. Demystifying animal models of adverse pregnancy outcomes: touching bench and bedside. Am J Reprod Immunol. 2013;69:567–584. [PubMed: 23448345]
22. Richardson L, Kim S, Menon R, Han A. Organ-on-chip technology: the future of feto-maternal interface research? Front Physiol. 2020;11.
23. Richardson L, Jeong S, Kim S, Han A, Menon R. Amnion membrane organ-on-chip: an innovative approach to study cellular interactions. FASEB J. 2019;33:8945–8960. [PubMed: 31039044]
24. Richardson L, Gnecco J, Ding T, et al. Fetal Membrane Organ-On-Chip: An Innovative Approach to Study Cellular Interactions, Reproductive Sciences. 2020;27:1562–1569. [PubMed: 32430706]
25. Herbst-Kralovetz MM, Quayle AJ, Ficarra M, et al. Quantification and comparison of toll-like receptor expression and responsiveness in primary and immortalized human female lower genital tract epithelia. Am J Reprod Immunol. 2008;59:212–224. [PubMed: 18201283]
26. Tantengco OAG, Richardson LS, Menon R. Effects of a gestational level of estradiol on cellular transition, migration, and inflammation in cervical epithelial and stromal cells. Am J Reprod Immunol. 2020. e13370
27. Dixon CL, Richardson L, Sheller-Miller S, Saade G, Menon R. A distinct mechanism of senescence activation in amnion epithelial cells by infection, inflammation, and oxidative stress. Am J Reprod Immunol. 2018;79:1–8.
28. Romero R, Roslansky P, Oyarzun E, et al. Labor and infection: II. Bacterial endotoxin in amniotic fluid and its relationship to the onset of preterm labor. Am J Obstet Gynecol. 1988;158:1044–1049. [PubMed: 3369483]
29. Richardson LS, Taylor RN, Menon R. Reversible EMT and MET mediate amnion remodeling during pregnancy and labor. Sci Signal. 2020;13:1–17.
30. Jin J, Richardson L, Sheller-Miller S, Zhong N, Menon R. Oxidative stress induces p38MAPK-dependent senescence in the feto-maternal interface cells. Placenta. 2018;67:15–23. [PubMed: 29941169]
31. Ruder B, Atreya R, Becker C. Tumour Necrosis Factor Alpha in Intestinal Homeostasis and Gut Related Diseases, International Journal of Molecular Sciences. 2019;20:1887.

Author Manuscript Author Manuscript Author Manuscript Author Manuscript

32. Huh D, Seo J. Systems and Methods for Producing Micro-engineered Models of the Human Cervix. US Patent App. 15/769,387; 2018.
33. Khorsandi D, Palacios S, Gaslain Y, et al. P159 Human uterine cervix-on-a-chip: establishing the first in vitro model to study the development of cervical carcinoma and human papiloma virus mechanism of action. Int J Gynecol Cancer. 2019;29:A155–A156.
34. Nott JP, Bonney EA, Pickering JD, Simpson NAB. The structure and function of the cervix during pregnancy. Transl Res Anat. 2016;2:1–7.
35. Romero R, Espinoza J, Kusanovic JP, et al. The preterm parturition syndrome. BJOG An Int J Obstet Gynaecol. 2006;113:17–42.
36. Maymon E, Ghezzi F, Edwin SS, et al. The tumor necrosis factor α and its soluble receptor profile in term and preterm parturition. Am J Obstet Gynecol. 1999;181:1142–1148. [PubMed: 10561634]
37. Romero R, Mazor M, Sepulveda W, Avila C, Copeland D, Williams J. Tumor necrosis factor in preterm and term labor. Am J Obstet Gynecol. 1992;166:1576–1587. [PubMed: 1595815]
38. Potter NT, Kosuda L, Bigazzi PE, et al. Relationships among cytokines (IL-1, TNF, and IL-8) and histologic markers of acute ascending intrauterine infection. J Matern Neonatal Med. 1992;1:142–147.
39. Velez DR, Fortunato SJ, Morgan N, et al. Patterns of cytokine profiles differ with pregnancy outcome and ethnicity. Hum Reprod. 2008;23:1902–1909. [PubMed: 18487217]
40. Battaglia RA, Delic S, Herrmann H, Snider NT. Vimentin on the move: new developments in cell migration. F1000Research. 2018;7:1796.
41. Lavenus SB, Tudor SM, Ullo MF, Vosatka KW, Logue JS. A flexible network of vimentin intermediate filaments promotes migration of amoeboid cancer cells through confined environments. J Biol Chem. 2020;295:6700–6709. [PubMed: 32234762]
42. Blander JM. Death in the intestinal epithelium—basic biology and implications for inflammatory bowel disease. FEBS J. 2016;283:2720–2730. [PubMed: 27250564]
43. Sedger LM, McDermott MF. TNF and TNF-receptors: from mediators of cell death and inflammation to therapeutic giants - past, present and future. Cytokine Growth Factor Rev. 2014;25:453–472. [PubMed: 25169849]

Author Manuscript Author Manuscript Author Manuscript Author Manuscript

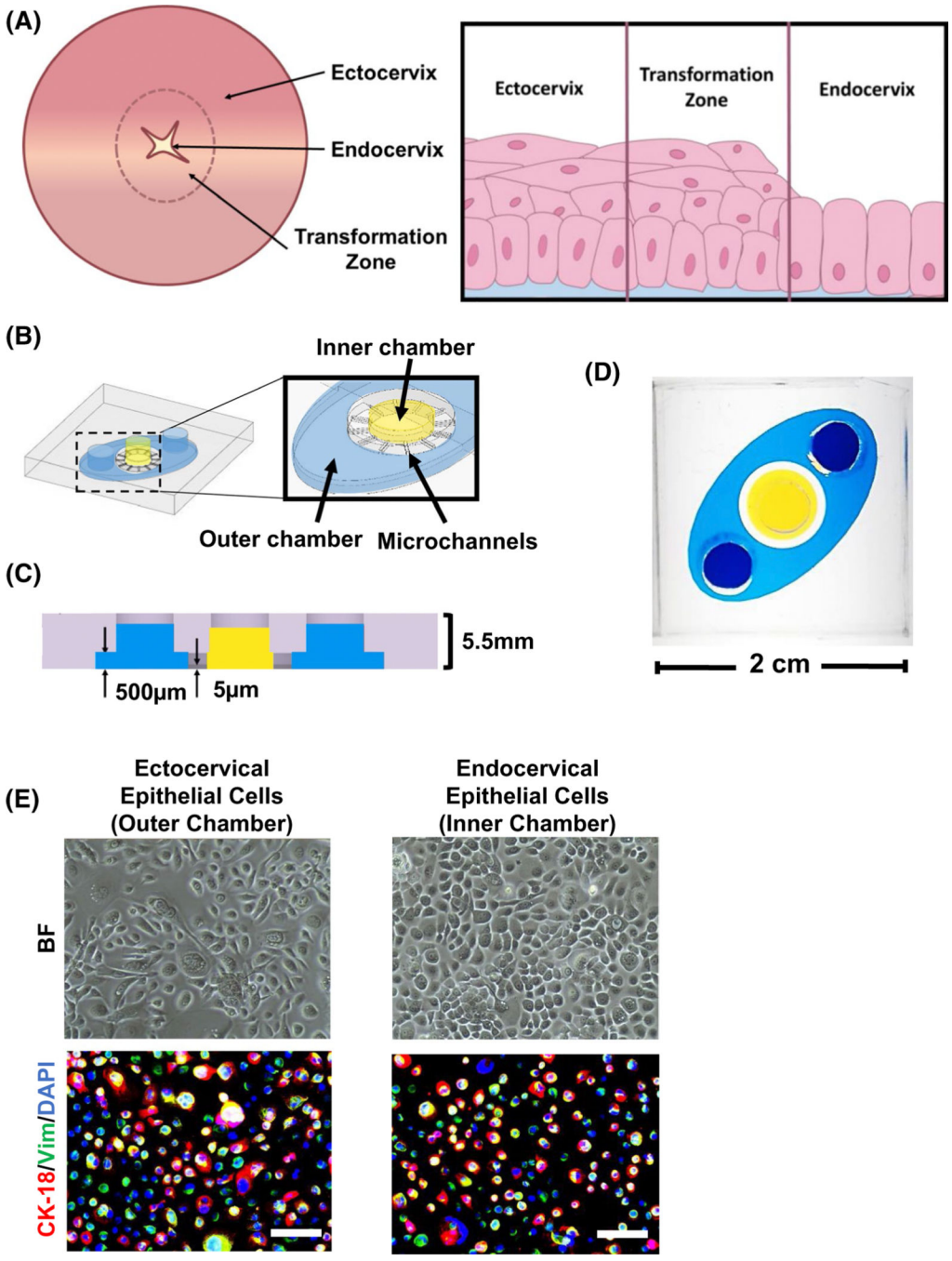

FIGURE 1.

CE-OOC design and cell culture within. The CE-OOC is designed to recapitulate the cervical epithelial layer in vitro by co-culturing ectocervical and endocervical epithelial cells separated by type IV collagen-filled microfluidic channels through which cells can migrate to form the transformation zone epithelium of the cervix. A, Schematic representation of the anatomy of the cervical epithelial layer. Left: gross morphology view; right: cross-sectional view. B, The CE-OOC design shown in 3D, where the two cell culture chambers separated by 24 shallow microchannels. C, Cross-sectional view showing the height difference

Author Manuscript Author Manuscript Author Manuscript Author Manuscript

between the cell culture chambers (500 μm height) and the microchannels (5 μm height). D, An image of the CE-OOC device showing the outer ectocervical epithelial cell culture chamber filled with blue color dye and the inner endocervical epithelial cell culture chamber filled with yellow color dye. E, Bright-field and fluorescence microscopy images of the ectocervical epithelial and endocervical epithelial cell cultures in the CE-OOC, showing cell morphology as well as CK-18 (red) and vimentin (green) expression. Nuclei are stained blue (DAPI: 4′,6-diamidino-2-phenylindole). Scale bar = 500 μm

Author Manuscript Author Manuscript Author Manuscript Author Manuscript

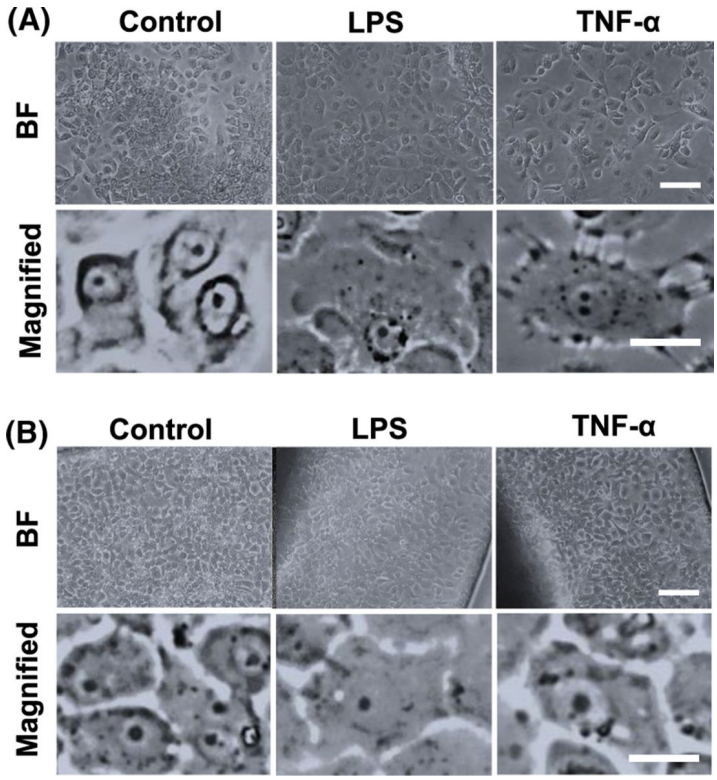

FIGURE 2.

Monocultured ectocervical and endocervical epithelial cell morphology in the CE-OOC under LPS and TNFα treatments for 96 hours. Bright-field (BF) microscopy showing the morphology of A, ectocervical and B, endocervical epithelial cells in the CE-OOC monoculture under control, LPS, and TNFα treatment for 96 hours. Magnified images were shown to highlight the morphology of the cervical epithelial cells under normal, LPS-, and TNFα-treated conditions. Scale bar = 500 μm (top) and 100 μm (bottom)

Author Manuscript Author Manuscript Author Manuscript Author Manuscript

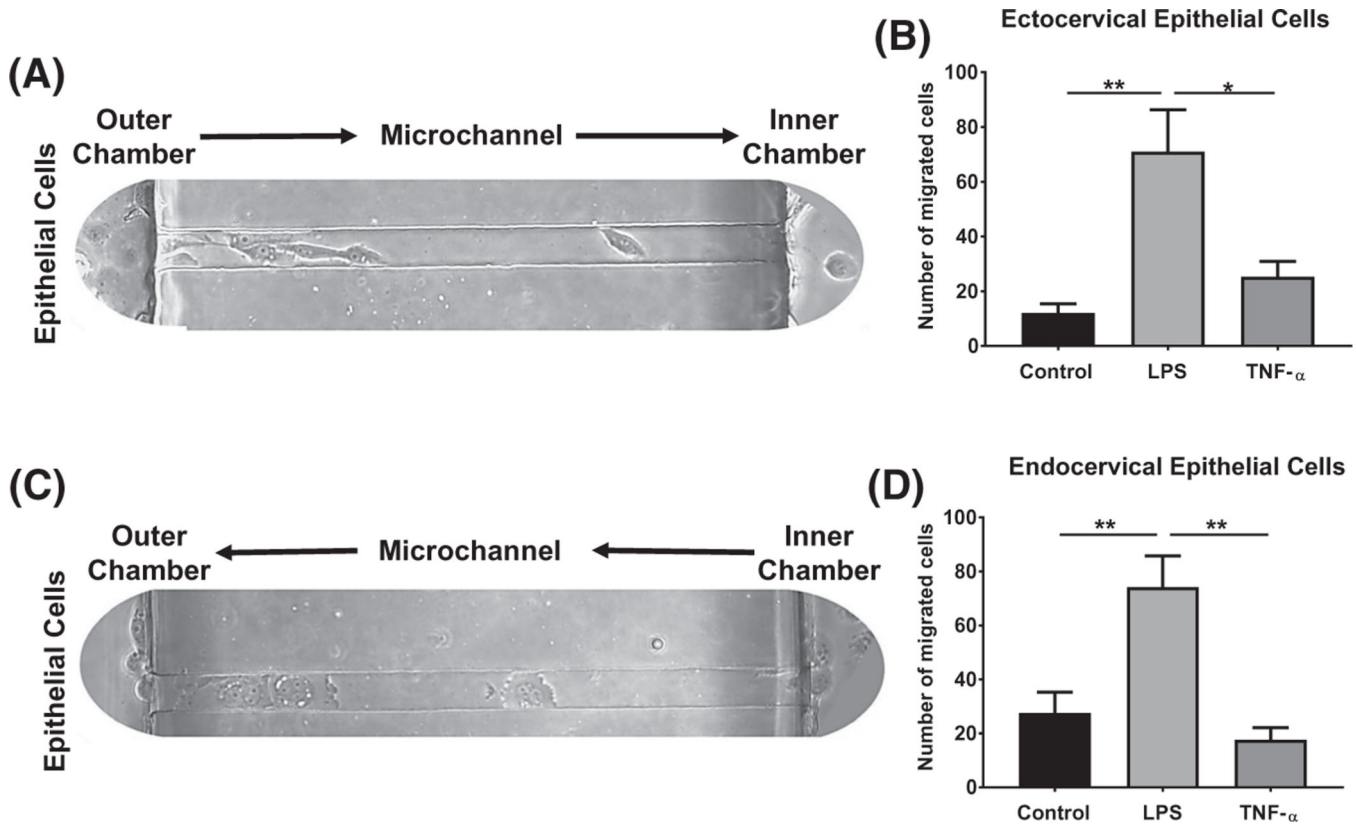

FIGURE 3.

Monocultured ectocervical and endocervical epithelial cell migration in the CE-OOC under control, LPS, and TNFα treatment conditions. Representative bright-field images and quantification of migrated monocultured ectocervical epithelial cells (A-B) and endocervical epithelial cells (C-D) in the CE-OOC device under control, LPS, and TNFα treatment conditions. Error bars represent mean ± SEM. n = 5 biological replicates. **P* < .05; ***P* < .01

Author Manuscript Author Manuscript Author Manuscript Author Manuscript

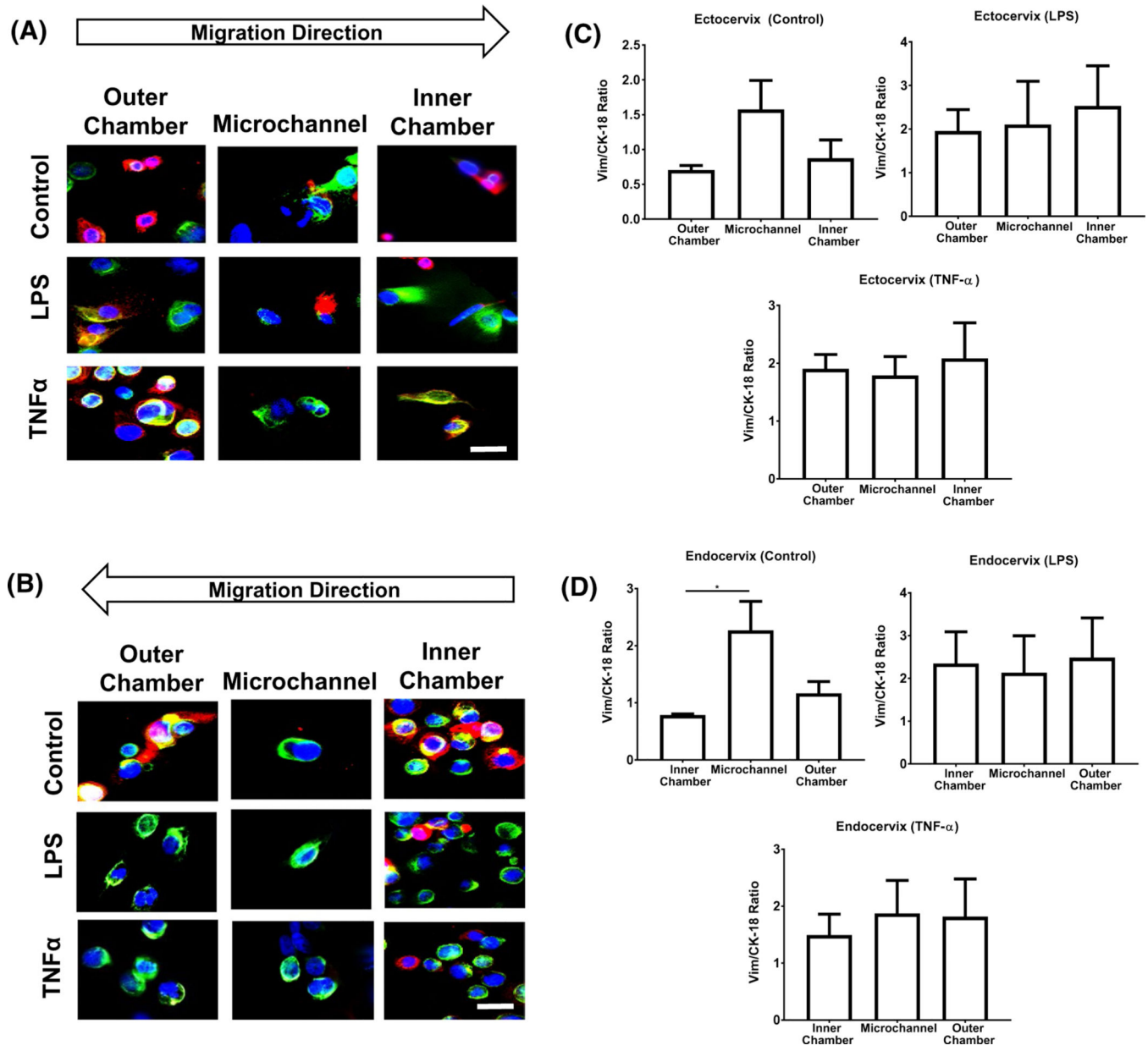

FIGURE 4.

Effects of LPS and TNFα treatment on cell transition and migration in the CE-OOC monoculture condition. Fluorescence microscopy images showing cell morphology, CK-18 (red), and vimentin (green) in the inner chamber, collagen-filled microchannels, and outer chamber of untreated (control), LPS-treated, and TNFα-treated ectocervical epithelial cells A, and endocervical epithelial cells B, Quantification of the ratio of vimentin and CK-18 relative fluorescence unit (RFU) in ectocervical C, and endocervical epithelial cells D, in the chambers and microchannels of the CE-OOC. Nuclei are stained blue (DAPI: 4′,6-diamidino-2-phenylindole). Scale bar = 50 μm. Error bars represent mean ± SEM. n = 9 technical replicates. A total of 5–10 cells per replicate were analyzed to calculate the average RFU of vimentin and CK-18 . $*P < .05$

Author Manuscript Author Manuscript Author Manuscript Author Manuscript

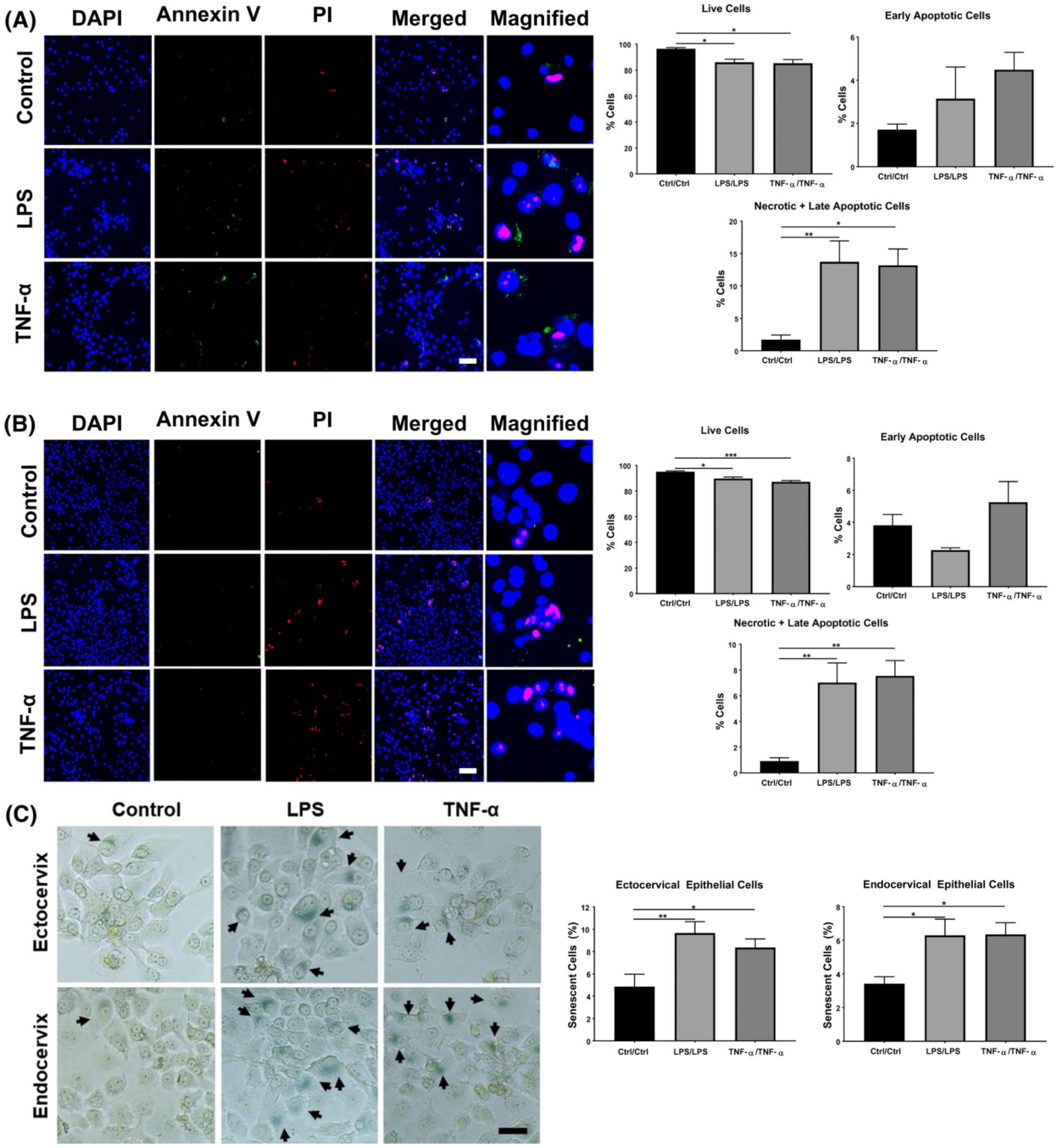

FIGURE 5.

Effect of LPS and TNFα on the cell fate in the CE-OOC co-culture condition. Annexin V (green) and propidium iodide (red) staining of untreated (control), LPS- and TNFα-treated co-culture of ectocervical epithelial cells A, and endocervical epithelial cells B, Nuclei are stained blue (DAPI: 4′,6-diamidino-2-phenylindole). Scale bar, 100 μm. Quantification of the percentage of cells that are viable, early apoptotic, late apoptotic, and necrotic in ectocervical epithelial cells (A) and endocervical epithelial cells (B). Error bars represent mean ± SEM. n = 5 technical replicates. C, Senescence-associated β-galactosidase (SA β-

Author Manuscript Author Manuscript Author Manuscript Author Manuscript

gal) staining in control and LPS- and TNFα-treated ectocervical epithelial cells and endocervical epithelial cells in CE-OOC co-culture. Arrows show the SA β-gal-positive cells. Scale bar, 100 μm. Quantification of senescent cells in control and LPS- and TNFα-treated ectocervical epithelial cells and endocervical epithelial cells in CE-OOC monoculture. Error bars represent mean ± SEM. n = 9 technical replicates. A total of 400–600 cells were analyzed per replicate of the apoptosis, necrosis, and senescence assays. *P < .05; **P < .01; and ***P < .001

Author Manuscript
Author Manuscript
Author Manuscript
Author Manuscript

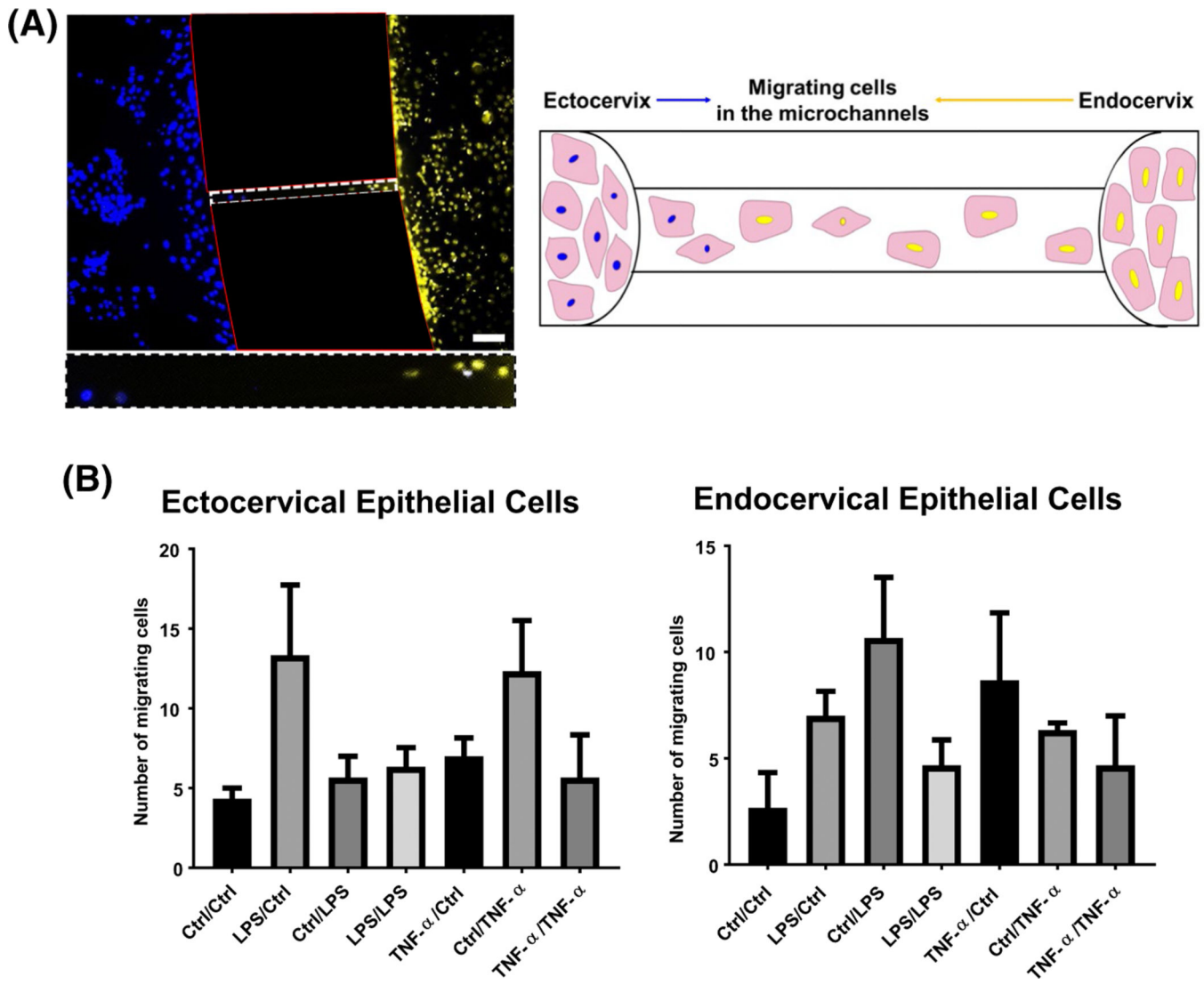

FIGURE 6.

Effect of LPS and TNFα on cell migration in the CE-OOC co-culture condition. A, Fluorescence microscopy of co-culture experiments showed that both ectocervical epithelial cells (blue) and endocervical epithelial cells (yellow) migrate through the collagen-filled microchannels. The bottom panel highlights the migrated ectocervical epithelial cells (blue) and endocervical epithelial cells (yellow) that have integrated into the microchannels. Scale bar, 200 μm. The right panel is a schematic representing the migration of cervical epithelial cells inside the microchannels. B, Quantification of migrating ectocervical epithelial cells that enter through collagen-filled microchannels. n = 3 biological replicates. C, Quantification of migrating endocervical epithelial cells that enter through the collagen-filled microchannels. Error bars represent mean ± SEM. n = 3 biological replicates

Author Manuscript Author Manuscript Author Manuscript Author Manuscript

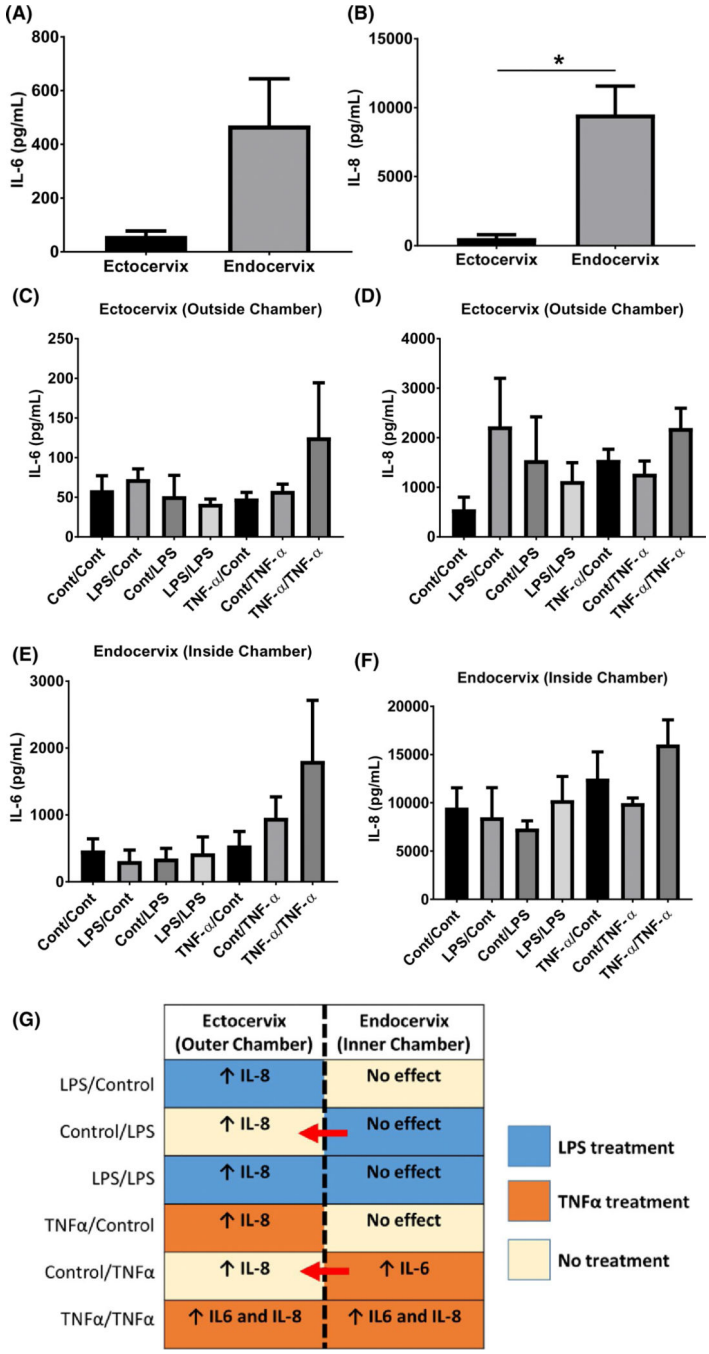

FIGURE 7.

Pro-inflammatory cytokine production and propagation in the CE-OOC co-culture systems. Luminex assay measured the baseline media concentrations of IL-6 and IL-8 from ectocervical (outer chamber) A, and endocervical epithelial cell media (inner chamber) B, For IL-6, ectocervical epithelial cells: 58.98 ± 18.21 pg/mL and endocervical epithelial cells: 470.6 ± 173.2 pg/mL. For IL-8, ectocervical epithelial cells: 556.1 ± 246 pg/mL and endocervical epithelial cells: 9515 ± 2048 pg/mL. C-D, IL-6 levels from ectocervical (C) and endocervical epithelial cell media (D) under control (untreated), LPS, and TNFα

Author Manuscript Author Manuscript Author Manuscript Author Manuscript

treatments. E-F, IL-8 levels from ectocervical (outer chamber) (E) and endocervical epithelial cell media (inner chamber) (F) under control (untreated), LPS, and TNFα treatment. G, Graphical summary of inflammatory cytokine production in the CE-OOC culture systems. The treatment of both chambers with TNFα promoted inflammation in both cervical epithelial cells, as supported by increased IL-6 and IL-8 production. Treatment in only one chamber also induced increased IL-8 production in the adjacent chamber indicating the propagation of inflammatory mediators in the CE-OOC. n = 5 biological replicates. The IL-6 and IL-8 levels were considered to be increased (↑) if there was a twofold change from the baseline (control/control) IL-6 and IL-8 levels. Otherwise, the result was classified as no change from baseline. *$P < .05$

Author Manuscript Author Manuscript Author Manuscript Author Manuscript

TABLE 1

Summary of co-culture treatments and abbreviations

Treatment	Outer chamber treatment (Ectocervix)	Inner chamber treatment (Endocervix)	Abbreviations
1	Control	Control	Control/Control
2	LPS	Control	LPS/Control
3	Control	LPS	Control/LPS
4	LPS	LPS	LPS/LPS
5	TNFα	Control	TNFα/Control
6	Control	TNFα	Control/TNFα
7	TNFα	TNFα	TNFα/TNFα

FASEB J. Author manuscript; available in PMC 2022 April 01.